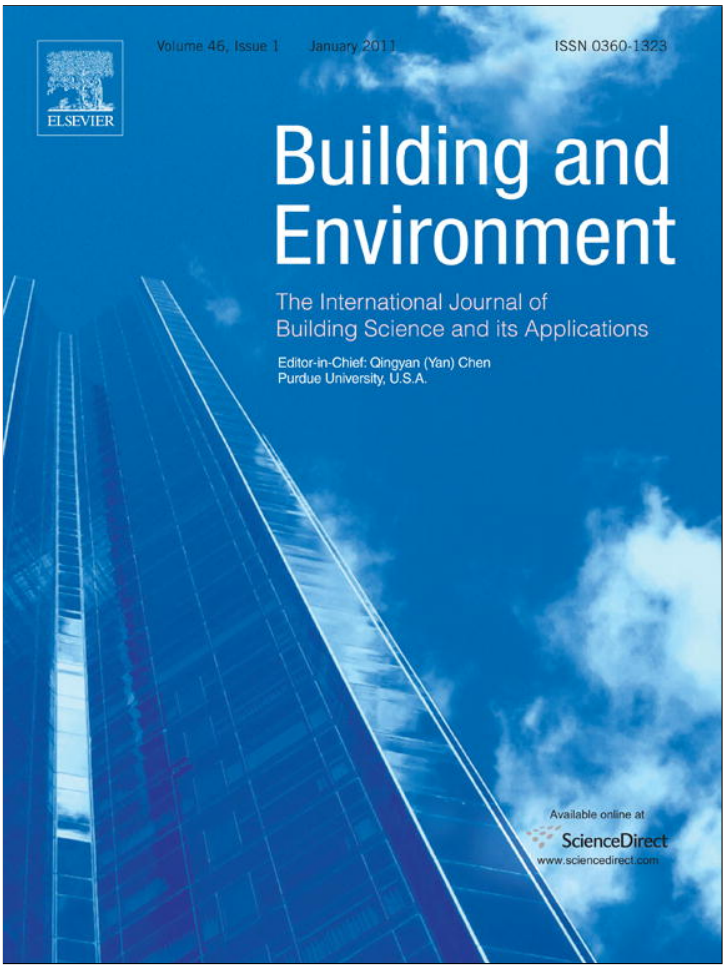

(This is a sample cover image for this issue. The actual cover is not yet available at this time.)

Building and Environment 49 (2012) 182–192

Contents lists available at SciVerse ScienceDirect

Building and Environment

journal homepage: www.elsevier.com/locate/buildenv

Uncertainty analysis and optimum concentration decay term for air exchange rate measurements: Estimation methods for effective volume and infiltration rate

Hiroyasu Okuyama*, Yoshinori Onishi[1]

Institute of Technology, Shimizu Corporation, 4-17 Etchujima 3-chome, Koto-ku, Tokyo 135-8530, Japan

ARTICLE INFO

Article history:
Received 7 July 2011
Received in revised form
9 September 2011
Accepted 15 September 2011

Keywords:
Air exchange rate
Concentration decay method
Least-squares method
Uncertainty propagation
Effective mixing volume
Discrepancy ratio

ABSTRACT

The widely used concentration decay method for measuring the single-zone air exchange rate has few limitations in its practical application, and several measurement standards employing this method have been published including ISO 12569, ASTM E741-95, and JIS A1406. These conventional methods, however, include several shortcomings that should be improved in terms of data analysis. Therefore, an equation for estimating the air exchange rate by the least-squares method from the number of points on the decay curve of the tracer gas and a method for determining the optimum decay term that minimizes the uncertainty are deduced. The method for calculating the standard deviation of uncertainty is also reconsidered and a new equation is deduced and verified. Furthermore, a method is introduced and verified for evaluating whether the premises of the measurement are sufficiently satisfied, such as the invariability of the air exchange rate and the uniformity of the tracer gas in the zone. In addition, a method for simultaneously estimating the effective mixing volume and the infiltration rate separately would be useful and is deduced. This estimation method's accuracy, which depends on the waveform and frequency of gas emission, is investigated through numerical experiments.

1. Introduction

Building air exchange and infiltration rates are significant factors in many aspects of building performance, including air-conditioning energy consumption, indoor air quality, and condensation. In most cases, however, actual air flow rates are different from the intentions of design and operation because of various factors; consequently, on-site measurement methods remain important technologies.

Direct measurements of air flow rate performed in the immediate vicinity of ventilation installations are insufficient for evaluating actual air exchange rate because shortcuts, bypasses, and leaks in the intake and exhaust routes, not to mention building envelope infiltration, may be present. A measurement method that is better suited to the actual situation is to use the tracer gas concentration to estimate the air exchange rates. There are various air exchange rate measurement methods that employ tracer gas. In general, the indoor air quality will likely differ among the zones within a structure, the application of a multi-zonal air flow rates measurement is preferable, but such methods have not yet been sufficiently disseminated.

In most current cases, doors between zones are left open and mixing fans are used to realize a uniform concentration of tracer gas throughout the building, or, conversely, the doors to the next rooms from the measurement room are sealed to create a single zone. The single-zone concentration decay method is highly practical because it allows for any method of tracer gas emission to be used, requires relatively simple equipment, and can be performed with only a minimal level of data analysis, making it the most widely used method.

Many researchers have been working on the uncertainty or error analysis of air infiltration rate measurements and effective mixing volume estimations. For example, Sherman et al. [1] derived a qualitative error analysis for tracer gas mixing problems, and also examined the question of effective mixing volume. Shaw [2] experimentally compared the effect of tracer gas type on the accuracy of air change measurements. Sandberg and Blomqvist [3] presented a quantitative estimate of the error of decay and constant concentration methods. D'Ottavio and Dietz [4] explored the errors resulting from treating a house as a well-mixed single volume, despite the actual situation being more similar to a two-zone case when a basement is included. D'Ottavio et al. [5] developed mathematical schemes estimating ventilation flows and their associated errors using a multiple perfluorocarbon tracer method. The relevant problems exist also in multi-zonal models that have been examined by many researchers, including the present authors.

* Corresponding author. Tel.: +81 3 3820 6438; fax: +81 3 3820 5955.
E-mail addresses: okuyama@shimz.co.jp (H. Okuyama), ohnishi@shimz.co.jp (Y. Onishi).
[1] Tel.: +81 3 3820 6439; fax: +81 3 3820 5955.

0360-1323/$ – see front matter © 2011 Elsevier Ltd. All rights reserved.
doi:10.1016/j.buildenv.2011.09.018

O'Neill and Crawford [6] proposed a recursive least-squares identification algorithm estimating flows and volumes using single tracer gas released by impulse.

In least-squares uncertainty analyses, in order to calculate the expectation of the regression equation error, not only the measurement uncertainty but also the regression equation residual, which includes various other causes of uncertainty, would be utilized. Furthermore, the formulation of uncertainty propagation to the estimated parameters would be also improved.

Almost all tracer gas emission methods described have used decay, square, or impulse emissions. Sinusoidal methods have been insufficiently investigated, however, despite it being well known that any periodic function can be represented by a series of trigonometric functions known as a Fourier series. We therefore investigate the effects of the use of a basic sinusoidal wave.

Even in a single-zone infiltration measurement, to consider the unfavorable influence of tracer gas concentration non-uniformity or to estimate the effective volume, we must consider the single zone using a subdivided multi-zonal model. In a spatially discrete diffusing system model, a finely discretized model with many nodes is generally required for high-frequency excitation, while a rough model with fewer nodes is sufficient for low-frequency excitation. Consequently, we should investigate the relation between the roughness of the model and the period of the sinusoidal excitation.

Furthermore, some measurement methods utilize ordinary differential equations of gas concentration for every short time interval Δt as a regression equation, especially where the time differential term tends to produce high-frequency noise because of, for example, measurement uncertainty. The least-squares method is easily affected by such unfavorable noise, making it necessary to preprocess the time series measurement data by using a low-pass filter.

Measurement uncertainty analysis is important in various fields, making standardization also important. A guide produced by the working group of the Joint Committee for Guides in Metrology (JCGM/WG 1) [7] can be referenced as an example of such standardization. In that paper, however, the parameter estimation, example uses only the arithmetic average, which is likely inferior to the more generic and useful least-squares method.

Several other standards have been published, including ISO 12569 [8] and ASTM E741-95 [9], as well as JIS A1406 in Japan [10]. Each of these standards includes measurement data analysis methods described in an informative annex.

However, these measurement standards share the following points (a)–(d), and the aforementioned measurement methods for simultaneously estimating effective mixing volume and infiltration rate include the following points (d)–(g), each of which require improvement or reconsideration.

(a) *Simultaneous least-squares solutions*
There is an equation for estimating the air exchange rate N from two measurement values on the tracer gas decay curve. But for utilizing more values, those standards describe a graphical method whereby the values are plotted on a logarithmic scale to find a linear fit, and suggest the utilization of some ready-made least-squares computer program.

(b) *Optimum term of concentration decay*
Some of the standards determine an appropriate measurement term by using the ratio of decaying concentration to the initial concentration. However, the basis for doing so is not clarified from the viewpoint of statistical uncertainty analysis. One can presume that an overly long or overly short term will have a deleterious effect due to the concentration measurement uncertainty. In this paper, we will numerically solve the nonlinear optimization problem, thus obtaining a curve that determines the optimum decay term.

(c) *Standard deviation of uncertainty*
The equation for the standard deviation of air exchange rate uncertainty (E_N) under conventional methods and the equation for the standard deviation (σ_N) deduced from the uncertainty propagation equation in this paper have structural differences, and these differences require examination.

(d) *Verification of the fulfillment of measurement prerequisites*
Obtaining accurate estimates of air exchange rates depends on the fulfillment of measurement prerequisites, such as invariability of the air exchange rate and uniformity of the tracer gas concentration. The coefficient of determination (COD) of the least-squares method has been proposed as an evaluation index, but COD is insensitive, as its value can be close to 1 even in cases where prerequisites have not been sufficiently fulfilled. In this paper, therefore, we employ a new index, the discrepancy ratio β, as an improved index of measurement prerequisites [11].

(e) *Method for simultaneously estimating effective mixing volume and infiltration rate*
"Effective mixing volume" is defined in this paper by system identification as a parameter of the differential equation for changes in gas concentration [12]. It can therefore be assumed that this will vary with the waveform and frequency of gas emission, which is an excitation for system identification, and therefore will not necessarily agree with the geometric chamber volume.

(f) *Relationship between periods of the trigonometric series function for gas emission and the effective mixing volume*
Okuyama [12] initially tested a square wave excitation. Square waves can also be expanded as a trigonometric series and have high-frequency terms. The system identification of the single-zone effective mixing volume and the infiltration rate presented in this paper examines such periods by using a pseudo-non-uniform model that represents an uneven distribution of gas concentrations.

(g) *Low-pass filter for preprocessing measurement data*
In the present research the moving term average is tested as a low-pass filter.

2. Estimation and uncertainty evaluation of air exchange rate by the least-squares method

2.1. Regression and solution equations

The initial measurement concentration is written as $C(t_1) = C(0)$, where $t_1 = 0\,(h)$ is the initial time of the concentration decay curve. Elapsed time for the j-th subsequent concentration measurement is written as t_j (h), and the concentration at that time is written as $C(t_j)$. Taking the air exchange rate as $N\,(\mathrm{h}^{-1})$, the following equation can be derived from the analytical solution for the concentration decay curve:

$$\log_e C(t_j) = -N \cdot t_j + \log_e C(0) \tag{1}$$

The following equation defines the equation error e_j for the least squares. This defines the vector matrix representation y_j, $\mathbf{Z}j$, and $\mathbf{a}$ in the following equation.

$$\begin{aligned} e_j &= \log_e C(t_j) - \left[-N \cdot t_j + \log_e C(0) \right] \\ &= y_j - \begin{bmatrix} t_j & 1 \end{bmatrix} \cdot \begin{bmatrix} -N \\ \log_e C(0) \end{bmatrix} = y_j - \mathbf{Z}_j \cdot \mathbf{a} \end{aligned} \tag{2}$$

The following equation defines the least-squares evaluation function J_a for the vector **a**, which is composed of the air exchange rate N and the logarithm of the initial concentration. Here, n_p is the number of points within the total measurement time. If the measurement is simply to find the air exchange rate, then n_p can be 2 or greater. When uncertainty evaluation is to be performed, however, n_p should be as large as possible (at least 3). Note that the left superscript t indicates a transpose operation.

$$J_a = \sum_{j=1}^{np} {}^t e_j \cdot e_j = \sum_{j=1}^{np} {}^t\left(y_j - \mathbf{Z}_j \cdot \mathbf{a}\right) \cdot \left(y_j - \mathbf{Z}_j \cdot \mathbf{a}\right) \tag{3}$$

When J_a is differentiated with respect to **a** and solved for 0, the following equation is obtained for the optimal value of **a**. Note that a hat (^) above a variable indicates an estimated parameter.

$$\begin{aligned}\hat{\mathbf{a}} &= \begin{bmatrix} -N \\ \log_e(0) \end{bmatrix} = \left(\sum_{j=1}^{np} {}^t\mathbf{Z}_j \cdot \mathbf{Z}_j\right)^{-1} \cdot \left(\sum_{j=1}^{np} {}^t\mathbf{Z}_j \cdot y_j\right) \\ &= \begin{bmatrix} \sum_{j=1}^{np} t_j^2 & \sum_{j=1}^{np} t_j \\ \sum_{j=1}^{np} t_j & n_p \end{bmatrix}^{-1} \cdot \begin{bmatrix} \sum_{j=1}^{np} t_j \cdot \log_e C(t_j) \\ \sum_{j=1}^{np} \log_e C(t_j) \end{bmatrix} \\ &= \frac{1}{n_p \cdot \sum_{j=1}^{np} t_j^2 - \left(\sum_{j=1}^{np} t_j\right)^2} \begin{bmatrix} n_p & -\sum_{j=1}^{np} t_j \\ -\sum_{j=1}^{np} t_j & \sum_{j=1}^{np} t_j^2 \end{bmatrix} \cdot \begin{bmatrix} \sum_{j=1}^{np} t_j \cdot \log_e C(t_j) \\ \sum_{j=1}^{np} \log_e C(t_j) \end{bmatrix}\end{aligned} \tag{4}$$

The estimated value for the air exchange rate N is therefore obtained by the following equation.

$$\hat{N} = \frac{\left(\sum_{j=1}^{np} t_j\right) \cdot \sum_{j=1}^{np} \log_e C(t_j) - n_p \cdot \sum_{j=1}^{np} t_j \cdot \log_e C(t_j)}{n_p \cdot \sum_{j=1}^{np} t_j^2 - \left(\sum_{j=1}^{np} t_j\right)^2} \tag{5}$$

In most cases $t_j = (j-1)\,\Delta t$ will be measured at equally spaced values for t, and in such cases the following comparatively simple equation can be used. Here, the term of concentration decay is $T = (n_p - 1)\,\Delta t$. Transformation to the following equation allows for the use of several formulas related to the sums of series.

$$\hat{N} = \frac{12}{n_p \cdot (n_p+1) \cdot T}\left[\sum_{j=1}^{np}\left\{\frac{(n_p-1)}{2} - (j-1)\right\} \cdot \log_e C\left\{\left(\frac{j-1}{n_p-1}\right) \cdot T\right\}\right] \tag{6}$$

2.2. Uncertainty propagation of concentration measurements and the optimum term of concentration decay

The variance of uncertainty for gas concentration measurements is written as σ_C^2. The uncertainty propagation law for the estimated error variance of the air exchange rate ${}_m\sigma_N^2$ is given below.

$${}_m\sigma_N^2 = \sigma_C^2 \cdot \sum_{j=1}^{np}\left(\frac{\partial \hat{N}}{\partial C(t_j)}\right)^2 \tag{7}$$

The following equation is obtained by differentiating Equation (6) with respect to $C(t_j)$.

$$\frac{\partial \hat{N}}{\partial C(t_j)} = \frac{12}{(n_p-1) \cdot n_p \cdot (n_p+1) \cdot \Delta t}\left\{\frac{(n_p-1)}{2} - (j-1)\right\}\frac{1}{C(t_j)} \tag{8}$$

Since in this case the decay model is taken to have no structural changes, we have the following equation.

$$C(t_j) = C(0) \cdot \exp\left(-\frac{(j-1)}{(n_p-1)}\,N \cdot T\right) \tag{9}$$

From Equations (8) and (9), Equation (7) can be written as follows.

$$\begin{aligned}{}_m\sigma_N^2 = {} & \frac{12^2 \cdot \sigma_c^2}{n_p^2 \cdot (n_p+1)^2 \cdot T^2 \cdot C(0)^2} \cdot \sum_{j=1}^{np}\left\{\frac{(n_p-1)}{2} - (j-1)\right\}^2 \\ & \cdot \exp\left\{\frac{2(j-1)}{(n_p-1)}\,N \cdot T\right\}\end{aligned} \tag{10}$$

Our goal here is to minimize the estimated error variance of this air exchange rate over the term of concentration decay T. We therefore differentiate with respect to T and solve the result for 0, giving the following equation.

$$\begin{aligned}\frac{\partial {}_m\sigma_N^2}{\partial T} = & -\frac{2 \cdot \sigma_c^2 \cdot 12^2}{n_p^2 \cdot (n_p+1)^2 \cdot T^3 \cdot C(0)^2} \\ & \cdot \left[\sum_{j=1}^{np}\left\{\frac{(n_p-1)}{2} - (j-1)\right\}^2 \cdot \exp\left\{\frac{2(j-1)}{(n_p-1)}\,N \cdot T\right\}\right. \\ & - N \cdot T \cdot \sum_{j=1}^{np}\frac{(j-1)}{(n_p-1)} \cdot \left\{\frac{(n_p-1)}{2} - (j-1)\right\}^2 \\ & \left. \cdot \exp\left\{\frac{2(j-1)}{(n_p-1)}\,N \cdot T\right\}\right] = 0\end{aligned} \tag{11}$$

From this equation, we take N and T as the lumped parameter NT, thus obtaining the following nonlinear equation.

$$\begin{aligned}f(NT) = & \sum_{j=1}^{np}\left\{\frac{(n_p-1)}{2} - (j-1)\right\}^2 \cdot \exp\left\{\frac{2(j-1)}{(n_p-1)}NT\right\} \\ & - NT \cdot \sum_{j=1}^{np}\frac{(j-1)}{(n_p-1)}\left\{\frac{(n_p-1)}{2} - (j-1)\right\}^2 \\ & \cdot \exp\left\{\frac{2(j-1)}{(n_p-1)}NT\right\} = 0\end{aligned} \tag{12}$$

Because this nonlinear equation for NT will change according to the number of measurement points n_p, we look for the optimum value of NT for each value of n_p ranging from 2 to approximately 300. We use Newton's method to solve the nonlinear equation. To do so, we use the following differential equation for NT.

$$\begin{aligned}\frac{\partial f(NT)}{\partial NT} = & \sum_{j=1}^{np}\frac{(j-1)}{(n_p-1)}\left\{\frac{(n_p-1)}{2} - (j-1)\right\}^2 \cdot \exp\left\{\frac{2(j-1)}{(n_p-1)}\,NT\right\} \\ & - NT \cdot \sum_{j=1}^{np}\frac{2(j-1)^2}{(n_p-1)^2}\left\{\frac{(n_p-1)}{2} - (j-1)\right\}^2 \\ & \cdot \exp\left\{\frac{2(j-1)}{(n_p-1)}\,NT\right\}\end{aligned} \tag{13}$$

When adding a corrective value δNT to an assumed NT yields a solution, the following equation gives an approximation of the first term in the Taylor expansion for the assumed value $NT + \delta NT$.

This becomes a recurrence relation for which iterative calculation approaches a solution.

$$f(NT+\delta NT) \cong f(NT)+\frac{\partial f(NT)}{\partial NT}\cdot\delta NT = 0 \tag{14}$$

A value slightly larger than 1 is used as the initial value. The optimal value for NT found in this way is written as $N\cdot T_m$, and Fig. 1 shows its curve. The resulting value is 1.108858 for both 2 and 3 points, but 1.132035 for 4 points, and 1.150974 for 5 points. As the total number of points increases, the value approaches approximately 1.25. The figure also includes for clarity a table of values for 1 to 60 points, for which changes are large.

2.3. Usage of the optimized curve

Here, we describe examples of using the optimized curve. When using air sampling bags to measure the tracer gas concentration several times during the decay process, we can assume the number of samples n_p and optimum NT_m will be obtained from the table in Fig. 1. First, we assume the extent of the air exchange rate broadly from N_s to N_l, and obtain the extent of the corresponding optimum decay term from T_l to T_s by NT_m. The first sampling time should be defined as zero. Other sampling times should be as equally spaced as possible, including the extent from T_l to T_s.

For continuous measurements, the number n_p is almost always large and the optimum NT_m is about 1.25. By assuming the broadly predicted extent of the air exchange rate from N_s to N_l, the corresponding extent of the optimized decay terms from T_l to T_s are obtained using NT_m. The measurement should be performed at least until T_s. The average term of T_l and T_s is regarded as the first assumed optimized decay term, and from this the air exchange rate is computed. Using this computed air exchange rate, the optimized decay term is next obtained using NT_m and the next air exchange rate is computed. This procedure is repeated until convergence is observed.

2.4. Propagation from regression equation error

There are two estimated parameters, the elements $[-N]$ and $[\log_e C(0)]$ of vector $\mathbf{a}$. The following equation gives the variance/covariance matrix $\mathbf{\Lambda}_a$. Here, $E(\ )$ represents a stochastic expectation operation.

$$\begin{aligned}\mathbf{\Lambda}_a &= E\{(\hat{\mathbf{a}}-E(\hat{\mathbf{a}}))\cdot{}^t(\hat{\mathbf{a}}-E(\hat{\mathbf{a}}))\} = \begin{bmatrix}\sigma_N^2 & \sigma^2_{N\cdot\log_e C(0)}\\ \sigma^2_{N\cdot\log_e C(0)} & \sigma^2_{\log_e C(0)}\end{bmatrix}\\ &= \left(\sum_{j=1}^{np}{}^t\mathbf{Z}_j\cdot\mathbf{Z}_j\right)^{-1}\cdot\left(\sum_{j=1}^{np}{}^t\mathbf{Z}_j\cdot E(e_j\cdot{}^te_j)\cdot\mathbf{Z}_j\right)\\ &\quad\cdot{}^t\left\{\left(\sum_{j=1}^{np}{}^t\mathbf{Z}_j\cdot\mathbf{Z}_j\right)^{-1}\right\} = \frac{E(e_j\cdot{}^te_j)}{n_p\cdot\sum_{j=1}^{np}t_j^2-\left(\sum_{j=1}^{np}t_j\right)^2}\\ &\quad\cdot\begin{bmatrix}n_p & -\sum_{j=1}^{np}t_j\\ -\sum_{j=1}^{np}t_j & \sum_{j=1}^{np}t_j^2\end{bmatrix}\end{aligned} \tag{15}$$

The variance of uncertainty σ_N^2 for air exchange rate N is element (1, 1) of the matrix in Equation (15), and is given by the following equation.

$$\sigma_N^2 = \frac{n_p\cdot E(e_j\cdot{}^te_j)}{n_p\cdot\sum_{j=1}^{np}t_j^2-\left(\sum_{j=1}^{np}t_j\right)^2} \tag{16}$$

2.5. Propagation from regression residual

Failure to establish the premises for measurement (independence from the effects of other zones, uniformity of gas concentration within a single zone, invariability for air exchange rate, etc.) can give rise to a large residual in Equation (1). Uncertainty in gas concentration measurements will also give rise to a residual. We therefore use the residual as starting point. To

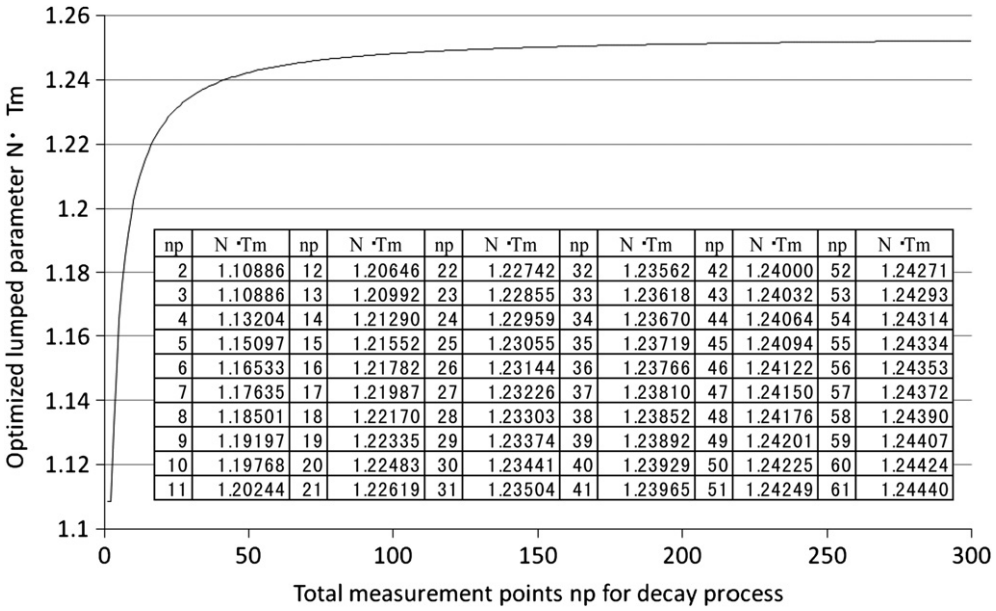

np	N ·Tm	np	N ·Tm	np	N ·Tm	np	N ·Tm	np	N ·Tm	np	N ·Tm
2	1.10886	12	1.20646	22	1.22742	32	1.23562	42	1.24000	52	1.24271
3	1.10886	13	1.20992	23	1.22855	33	1.23618	43	1.24032	53	1.24293
4	1.13204	14	1.21290	24	1.22959	34	1.23670	44	1.24064	54	1.24314
5	1.15097	15	1.21552	25	1.23055	35	1.23719	45	1.24094	55	1.24334
6	1.16533	16	1.21782	26	1.23144	36	1.23766	46	1.24122	56	1.24353
7	1.17635	17	1.21987	27	1.23226	37	1.23810	47	1.24150	57	1.24372
8	1.18501	18	1.22170	28	1.23303	38	1.23852	48	1.24176	58	1.24390
9	1.19197	19	1.22335	29	1.23374	39	1.23892	49	1.24201	59	1.24407
10	1.19768	20	1.22483	30	1.23441	40	1.23929	50	1.24225	60	1.24424
11	1.20244	21	1.22619	31	1.23504	41	1.23965	51	1.24249	61	1.24440

Fig. 1. Relation between optimized lumped parameter $N\cdot T_m$ and total measurement points.

calculate residuals, we need the following estimate of the log of the initial concentration, derived from Equation (4).

$$\log_e \hat{C}(0) = \frac{\left(\sum_{j=1}^{np} t_j^2\right)\cdot\sum_{j=1}^{np}\log_e C(t_j) - \left(\sum_{j=1}^{np} t_j\right)\cdot\left(\sum_{j=1}^{np} t_j\right)\cdot\log_e C(t_j)}{n_p\cdot\sum_{j=1}^{np} t_j^2 - \left(\sum_{j=1}^{np} t_j\right)^2} \tag{17}$$

The residual ${}_a\varepsilon_j$ is calculated as follows from regression equation (1). Here, ${}_a\varepsilon_j$ is the residual corresponding to the j-th measurement data.

$${}_a\varepsilon_j = \log_e C(t_j) + \hat{N}\cdot t_j - \log_e \hat{C}(0) \tag{18}$$

The expected value for the equation error $E({}_e j\cdot {}^t e_j)$ is calculated as the average of the residuals. The variance of uncertainty ${}_r\sigma_N^2$ from this residuals is calculated by Equation (20), substituting Equation (19) into Equation (16). Because Equation (20) is structurally different from the equation used in conventional methods, we can expect different results.

$${}_a\hat{\varepsilon}^2 = \frac{1}{(n_p-2)}\cdot\sum_{j=1}^{np} {}_a\varepsilon_j^2 \tag{19}$$

$${}_r\sigma_N^2 = \frac{n_p\cdot {}_a\hat{\varepsilon}^2}{n_p\cdot\sum_{j=1}^{np} t_j^2 - \left(\sum_{j=1}^{np} t_j\right)^2} \tag{20}$$

Confidence intervals can be calculated from the variance. Note that the variance from measurement uncertainty ${}_m\sigma_N^2$ has already been described by Equation (10).

2.6. Coefficient of determination

Next, we derive the coefficient of determination COD. Equation (21) calculates the sum of residual squares $s(N)$. Equation (22) calculates the total variation s_y. Equation (23) calculates the COD, based on the sum of residual squares and the total variation.

$$s(\hat{N}) = \sum_{j=1}^{np} {}_a\varepsilon_j^2 = \sum_{j=1}^{np}\left\{\log_e C(t_j) + \hat{N}\cdot t_j - \log_e \hat{C}(0)\right\}^2 \tag{21}$$

$$\begin{aligned} s_y &= \sum_{j=1}^{np} y_j^2 - \frac{1}{n_p}\cdot\left(\sum_{j=1}^{np} y_j\right)^2 \\ &= \sum_{j=1}^{np}\left[\log_e C(t_j)\right]^2 - \frac{1}{n_p}\cdot\left[\sum_{j=1}^{np}\log_e C(t_j)\right]^2 \end{aligned} \tag{22}$$

$$\mathrm{COD} = 1 - \frac{s(\hat{N})}{s_y} \tag{23}$$

2.7. Discrepancy ratio β of model premises

If the variance of uncertainty ${}_r\sigma^2{}_N$ from the residual error of Equation (20) is large as compared with the variance of uncertainty ${}_m\sigma^2{}_N$ of Equation (10), which depends only on measurement uncertainty of the gas concentration, then there is likely a significant gap between the premises of the mathematical model and actual conditions. The following equation uses the standard deviation of each to define β [11] as the discrepancy ratio of the model premises.

$$\beta_N = \frac{{}_r\sigma_N}{{}_m\sigma_N} \tag{24}$$

If β is considerably larger than 1, then there is a possibility that the infiltration rate changed, that concentration uniformity within the zone was not maintained, or gas leaked between the adjacent zones. In such a case, the measurement conditions will likely need to be modified, and the measurement repeated.

3. Simultaneous estimation of effective mixing volume and infiltration rate

3.1. Basic differential and regression equations

Deriving the change in gas concentration $c(t)$ ($\mathrm{mg\cdot m^{-3}}$) from the gas release rate $g(t)$ ($\mathrm{mg\cdot h^{-1}}$) allows separate estimation of the infiltration rate q ($\mathrm{m^3\cdot h^{-1}}$) and the effective mixing volume v ($\mathrm{m^3}$) from these measurements. The method used is an application of dispersive system parameter identification theory [12] to the simple case of a single zone.

The tracer gas is taken as being emitted with variation according to a square or sinusoidal waveform. Exterior concentration of the gas is given as $c_o(t)$ so that gasses such as carbon dioxide that exist externally can be accommodated. The differential equation for variation in gas concentration is as follows. Here, the dot over the variable c indicates a time derivative.

$$v\cdot\dot{c}(t) = q\cdot(c_o(t) - c(t)) + g(t) \tag{25}$$

This can be transformed to the following equation for vector $\mathbf{p}$, which contains the parameters v and q to be estimated. We therefore define the row matrix $\mathbf{U}(t)$ and rewrite the equation as follows.

$$g(t) = \left[\dot{c}(t), c(t) - c_o(t)\right]\cdot\begin{bmatrix} v \\ q \end{bmatrix} = \mathbf{U}(t)\cdot\mathbf{p} \tag{26}$$

The changes in $g(t)$, $c(t)$, and $c_o(t)$ are measured at each Δt. These variables are calculated as an integral linear interpolation over $(k-1)\Delta t$ to $k\Delta t$, and are defined by g_k, d_k, and c_k,.

$$g_k = \int_{(k-1)\Delta t}^{k\Delta t} g(t)dt \cong \{g(k\Delta t) + g((k-1)\Delta t)\}\cdot\Delta t/2 \tag{27}$$

$$d_k = \int_{(k-1)\Delta t}^{k\Delta t} \dot{c}(t)dt \cong \{c(k\Delta t) - c((k-1)\Delta t)\} \tag{28}$$

$$\begin{aligned} c_k = \int_{(k-1)\Delta t}^{k\Delta t} \{c(t) - c_o(t)\}\mathrm{d}t &\cong \{c(k\Delta t) + c((k-1)\Delta t)\}\cdot\Delta t/2 \\ &- \{c_o(k\Delta t) + c_o((k-1)\Delta t)\}\cdot\Delta t/2 \end{aligned} \tag{29}$$

$\mathbf{U}_k$ is defined as follows.

$$\mathbf{U}_k = \int_{(k-1)\Delta t}^{k\Delta t} \mathbf{U}(t)\mathrm{d}t = [d_k, c_k] \tag{30}$$

From the above, the discrete time regression equation of Equation (25) becomes the following.

$$g_k = \mathbf{U}_k \cdot \mathbf{p} \tag{31}$$

3.2. Estimation equations for effective mixing volume and infiltration rate

To apply the least-squares method, the error from Equation (31) is defined as e_k by Equation (32). As was done above for Equation (3), the squares of e_k are summed over the total number of time steps nt, and taken as the evaluation function J_p. The optimal estimation for $\mathbf{p}$ is then calculated by differentiating J_p. with respect to $\mathbf{p}$ according to Equation (34).

$$e_k = g_k - \mathbf{U}_k \cdot \mathbf{p} \tag{32}$$

$$J_p = \sum_{k=1}^{nt} {}^t e_k \cdot e_k \tag{33}$$

$$\hat{\mathbf{p}} = \left[\sum_{k=1}^{nt} ({}^t\mathbf{U}_k \cdot \mathbf{U}_k)\right]^{-1} \cdot \left[\sum_{k=1}^{nt} {}^t\mathbf{U}_k \cdot g_k\right] \tag{34}$$

A second-order inverse matrix can be explicitly described, and therefore the optimal estimation of $\mathbf{p}$, too, can be explicitly described.

$$\begin{aligned}\hat{\mathbf{p}} = \begin{bmatrix} v \\ q \end{bmatrix} &= \begin{bmatrix} \sum_{k=1}^{nt} d_k^2 & \sum_{k=1}^{nt} d_k \cdot c_k \\ \sum_{k=1}^{nt} d_k \cdot c_k & \sum_{k=1}^{nt} c_k^2 \end{bmatrix}^{-1} \cdot \begin{bmatrix} \sum_{k=1}^{nt} d_k \cdot g_k \\ \sum_{k=1}^{nt} c_k \cdot g_k \end{bmatrix} \\ &= \frac{1}{\left(\sum_{k=1}^{nt} d_k^2\right)\left(\sum_{k=1}^{nt} c_k^2\right) - \left(\sum_{k=1}^{nt} d_k \cdot c_k\right)^2} \\ &\quad \cdot \begin{bmatrix} \sum_{k=1}^{nt} c_k^2 & -\sum_{k=1}^{nt} d_k \cdot c_k \\ -\sum_{k=1}^{nt} d_k \cdot c_k & \sum_{k=1}^{nt} d_k^2 \end{bmatrix} \cdot \begin{bmatrix} \sum_{k=1}^{nt} d_k \cdot g_k \\ \sum_{k=1}^{nt} c_k \cdot g_k \end{bmatrix}\end{aligned} \tag{35}$$

The estimated values for the effective mixing volume v and the infiltration rate q are therefore calculated as follows.

$$\hat{v} = \frac{\left(\sum_{k=1}^{nt} c_k^2\right) \cdot \left(\sum_{k=1}^{nt} d_k \cdot g_k\right) - \left(\sum_{k=1}^{nt} d_k \cdot c_k\right) \cdot \left(\sum_{k=1}^{nt} c_k \cdot g_k\right)}{\left(\sum_{k=1}^{nt} d_k^2\right) \cdot \left(\sum_{k=1}^{nt} c_k^2\right) - \left(\sum_{k=1}^{nt} d_k \cdot c_k\right)^2} \tag{36}$$

$$\hat{q} = \frac{\left(\sum_{k=1}^{nt} d_k^2\right) \cdot \left(\sum_{k=1}^{nt} c_k \cdot g_k\right) - \left(\sum_{k=1}^{nt} d_k \cdot c_k\right) \cdot \left(\sum_{k=1}^{nt} d_k \cdot g_k\right)}{\left(\sum_{k=1}^{nt} d_k^2\right) \cdot \left(\sum_{k=1}^{nt} c_k^2\right) - \left(\sum_{k=1}^{nt} d_k \cdot c_k\right)^2} \tag{37}$$

3.3. Propagation from regression equation error to variance of uncertainty for estimated parameters

As with Equation (15), propagation of uncertainty from regression equation errors to estimated parameters is considered, and the variance of uncertainty of the effective mixing volume σ_v^2 is calculated as shown below.

$$\begin{aligned}\mathbf{\Lambda}_{\mathbf{p}} &= E\{(\hat{\mathbf{p}} - E(\hat{\mathbf{p}})) \cdot {}^t(\hat{\mathbf{p}} - E(\hat{\mathbf{p}}))\} = \begin{bmatrix} \sigma_v^2 & \sigma_{v\cdot q}^2 \\ \sigma_{v\cdot q}^2 & \sigma_q^2 \end{bmatrix} \\ &= \left(\sum_{k=1}^{nt} {}^t\mathbf{U}_k \cdot \mathbf{U}_k\right)^{-1} \cdot \left(\sum_{k=1}^{nt} {}^t\mathbf{U}_k \cdot E(e_k \cdot {}^t e_k) \cdot \mathbf{U}_k\right) \\ &\quad \cdot {}^t\left\{\left(\sum_{k=1}^{nt} {}^t\mathbf{U}_k \cdot \mathbf{U}_k\right)^{-1}\right\} = \frac{E(e_k \cdot {}^t e_k)}{\left(\sum_{k=1}^{nt} d_k^2\right)\left(\sum_{k=1}^{nt} c_k^2\right) - \left(\sum_{k=1}^{nt} d_k \cdot c_k\right)^2} \\ &\quad \cdot \begin{bmatrix} \sum_{k=1}^{nt} c_k^2 & -\sum_{k=1}^{nt} d_k \cdot c_k \\ -\sum_{k=1}^{nt} d_k \cdot c_k & \sum_{k=1}^{nt} d_k^2 \end{bmatrix}\end{aligned} \tag{38}$$

$$\sigma_v^2 = \frac{E(e_k \cdot {}^t e_k) \cdot \left(\sum_{k=1}^{nt} c_k^2\right)}{\left(\sum_{k=1}^{nt} d_k^2\right) \cdot \left(\sum_{k=1}^{nt} c_k^2\right) - \left(\sum_{k=1}^{nt} d_k \cdot c_k\right)^2} \tag{39}$$

The variance of uncertainty of the infiltration rate σ_q^2 is calculated as follows.

$$\sigma_q^2 = \frac{E(e_k \cdot {}^t e_k) \cdot \left(\sum_{k=1}^{nt} d_k^2\right)}{\left(\sum_{k=1}^{nt} d_k^2\right) \cdot \left(\sum_{k=1}^{nt} c_k^2\right) - \left(\sum_{k=1}^{nt} d_k \cdot c_k\right)^2} \tag{40}$$

3.4. Two expected values of the regression equation error

Two types of expected values $E(e_k \cdot {}^t e_k)$ of the regression equation error can be considered. The first type is calculated from the residual ${}_p\varepsilon_k$, as defined below.

$${}_p\varepsilon_k = g_k - \mathbf{U}_k \cdot \hat{\mathbf{p}} \tag{41}$$

The sum of squares of these values is divided by the total time step count nt less the 2 degrees of freedom, and thus the expected value ${}_rE(e_k \cdot {}^t e_k)$ is calculated from the residuals as follows.

$${}_rE(e_k \cdot {}^t e_k) = \frac{1}{(nt-2)} \sum_{k=1}^{nt} {}_p\varepsilon_k \cdot {}^t_p\varepsilon_k \tag{42}$$

We will next derive the expected value for the regression error from measurement uncertainty, ${}_mE(e_k \cdot {}^t e_k)$. Here, σ_g is the standard deviation of the measurement uncertainty for the gas release rate g, and σ_c is the standard deviation of the measurement uncertainty for the gas concentrations c and c_o. The values of the integrals of the gas release rate and concentration at Δt, and that of the time derivative of the gas concentrations, are given in Equations (27), (29), and (28), respectively. The variance of uncertainty for each can be calculated from the uncertainty propagation law as follows.

$$\sigma_{gk}^2 = (1/2) \cdot \Delta t^2 \cdot \sigma_g^2 \tag{43}$$

$$\sigma_{dk}^2 = 2 \cdot \sigma_c^2 \tag{44}$$

$$\sigma_{ck}^2 = \Delta t^2 \cdot \sigma_c^2 \tag{45}$$

Once the least-squares method has been applied to estimates v and q, and Equations (43)–(45) have been used to obtain the variance of uncertainty, the expected value for error variance from the measurement uncertainty of regression equation (32), ${}_mE(e_k \cdot {}^t e_k)$, is calculated as follows.

$$\begin{aligned} {}_mE(e_k \cdot {}^t e_k) &= \left(\frac{\partial e_k}{\partial g_k}\right)^2 \cdot \sigma_{gk}^2 + \left(\frac{\partial e_k}{\partial d_k}\right)^2 \cdot \sigma_{dk}^2 + \left(\frac{\partial e_k}{\partial c_k}\right)^2 \cdot \sigma_{ck}^2 \\ &= \sigma_{gk}^2 + \hat{v}^2 \cdot \sigma_{dk}^2 + \hat{q}^2 \cdot \sigma_{ck}^2 \\ &= (1/2) \cdot \Delta t^2 \cdot \sigma_g^2 + \hat{v}^2 \cdot 2 \cdot \sigma_c^2 + \hat{q}^2 \cdot \Delta t^2 \cdot \sigma_c^2 \end{aligned} \quad (46)$$

3.5. Coefficient of determination COD and discrepancy ratio β

The coefficient of determination COD is also calculated similarly to Equations (21)–(23). The sum of squares of ${}_p\varepsilon_k$ in Equation (41) is taken as a sum of residual squares, and total variation is calculated taking g_k to correspond to y_j. For the effective mixing volume v and infiltration rate q, the standard deviations ${}_r\sigma_v$ and ${}_r\sigma_q$ originating from the residual, as well as the standard deviations ${}_m\sigma_v$ and ${}_m\sigma_q$ originating from the measurement uncertainty, are each calculated by using Equations (39) and (40), where $E(e_k \cdot {}^t e_k)$ is replaced by ${}_rE(e_k \cdot {}^t e_k)$ or ${}_mE(e_k \cdot {}^t e_k)$ given by Equations (42) and (46), respectively. Doing this allows calculation of the regression model premises discrepancy ratio β for v and q as follows.

$$\beta_v = \frac{{}_r\sigma_v}{{}_m\sigma_v} \quad (47)$$

$$\beta_q = \frac{{}_r\sigma_q}{{}_m\sigma_v} \quad (48)$$

If these ratios are significantly larger than 1, then there is a possibility that premises related to invariability, uniformity, or linearity were not fulfilled.

3.6. Gas emission waveforms and frequencies

The method of this paper is the special case of applying system identification theory [12] for a multi-nodal general diffusion system to a single-node system. In the initial development of the multi-chamber air flow rates measurement system, emission was performed as a square wave due to limitations related to the gas release equipment and the simplicity of its controller software.

In building heat transfer systems, however, appropriate temperature measurement within the wall or structural framework is difficult. This frequently gave poor results for system identification when models were constructed using only room air as nodes and electric heaters to generate square waveforms, as there were large discrepancies between the model and the actual state.

Several years of investigations, however, have revealed that satisfactory system identification results can be obtained, even in a rough model of heat transfer with few nodes, by generating heat in a smooth sinusoidal waveform over relatively long periods.

Square waveforms expanded into a trigonometric series include high frequency terms. In a rough system identification model tracing such terms is difficult, and likely to give poor results. However, the use of a period that is longer than changes in daily meteorological conditions is time consuming.

Even a single zone model with non-uniform gas concentration should allow for sufficient simulation of changes in concentration, if gas emission is performed in a long-wavelength sinusoidal pattern. The effective mixing volume v is considered to be a parameter dependent upon frequency.

3.7. Moving average as low-pass filter

Measurement uncertainty and the like frequently produce high-frequency noise in methods using the gas concentration ordinary differential equation for a short time interval Δt as a regression equation contributing to the least-squares summation. The least-squares method is easily influenced by such type of noise. Consequently, the time series measurement data requires some preprocessing by a low-pass filter. One of the simplest filters is a moving term average, which smoothes changes in the measurement data. The calculated each term average is placed at the center of the each term in the newly generated data.

Low-pass filters are also useful for diffusion system identification of building heat transfer systems. Building heat transfer system identification models tend to be rough (have few nodes), and so excitation periods should be rather long. The term of the moving average should be longer than the changing period of the noise, yet shorter than the excitation period. When using solar radiation as an identification excitation in addition to electric heaters, a one-hour moving average term may be appropriate. For thermally heavy buildings, however, even daily meteorological changes should be regarded as noise, and in these cases the appropriate term of the moving average may become very long. These periods can be determined using the discrepancy ratio β and the coefficient of determination COD.

4. Verification by numerical case studies

4.1. Verification of optimum term of concentration decay

According to the method of determining the optimum term of concentration decay presented in this paper, given, for example, an air exchange rate N of 0.5 ($1\ h^{-1}$), the optimum term of concentration decay for 2, 3 and 4 total measurements is 2.22, 2.22, and 2.26 h, respectively. As the number of measurements increases further, the optimal term approaches 2.5 h. We therefore examined how, for the term of concentration decay under consideration, the error in the results of estimating N varied when the term was changed from 0.5 to 9 h.

Because verification would require a large amount of data processing, we investigated cases where the number of decay curve measurement points was $n_p = 2$, 3, and 4. If we employ random number generation to add normal distribution error to the true analytical solution for gas concentration decay, the nature of random error would require calculations for an enormous number of cases to clearly reveal the trends of interest. We therefore added to the true values positive or negative values of the standard deviation for uncertainty, σ. The standard deviation for measurements of gas concentration σ_c was 0.2 ($mg \cdot m^{-3}$), and the standard deviation for gas release rate σ_g was 0.012 ($mg \cdot s^{-1}$).

In the case where $n_p = 2$ points, the errors added to the first and second points were either $+\sigma$ and $-\sigma$ or $-\sigma$ and $+\sigma$, respectively, giving two sets of data. Additions of $+\sigma$ and $+\sigma$ or $-\sigma$ and $-\sigma$ were not performed, as such error would be systematic. Similarly, for a case of n_p measurement points, we obtained $2^{np}-2$ measurement data sets. Namely, cases with $n_p = 2$, 3 and 4 measurements generated 2, 6, and 14 measurement data sets, respectively. Fig. 2 shows a graph of the average error for the estimated values of N from each case of n_p measurement points. Twenty-four cases were examined with the term of concentration decay ranging from 0.5

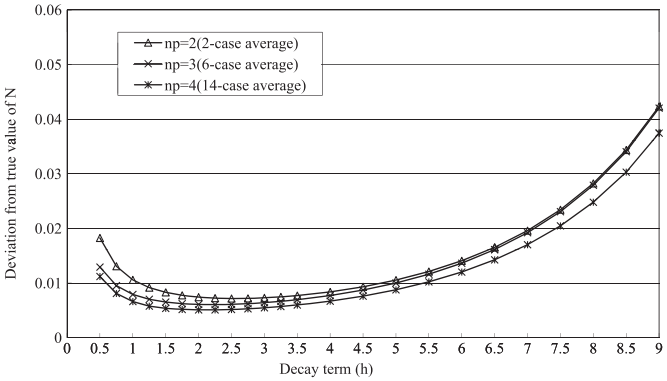

Fig. 2. Verification of optimized decay term.

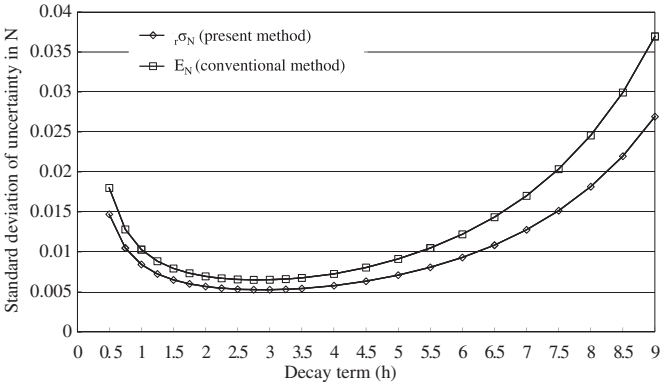

Fig. 4. Comparison of standard deviation of uncertainty in *N*.

to 9 h. Results show that the minimum value for estimated error of *N* were obtained at a term of concentration decay of around 2.2 h.

4.2. Air exchange rate for the decay method and uncertainty evaluation

The analytical solution for the tracer gas concentration decay curve was taken as the true measurement value. The true values for chamber volume, infiltration rate, and air exchange rate were taken to be 100 (m^3), 50 ($m^3 \cdot h^{-1}$), and 0.5 (h^{-1}), respectively. We first confirmed the results of estimation in the case of no measurement error and complete fulfillment of model premises. The trial calculation was performed where the term of concentration decay was the optimal 2.5 (h), Δt was 1 (min), the total number of time steps was 151, the gas used was SF_6, and initial concentration was approximately 50 ($mg \cdot m^{-3}$). The resulting estimated *N* was 0.500000 (h^{-1}), and COD for regression error due to error in the numerical calculation was 1.00000.

We next used measurement data to which uncertainty had been applied as described in the previous section. We then compared E_N, the standard deviation of uncertainty of *N* according to the conventional method, with $_r\sigma_N$, the standard deviation of uncertainty of the present method. When doing so, we used measurement data with a maximum of $n_p = 4$ measurement points on the decay curve. We furthermore examined measurement uncertainty after addition of the random values. As shown in Fig. 3, the frequency distribution of measurement uncertainty for 151 measurements closely followed a normal distribution curve. The standard deviation for these values was 0.2048, close to the presumed value 0.2.

Sixteen air exchange rates *N* and residual errors were obtained for each of the 24 terms of concentration decay, and the estimated value for standard deviation E_N (from the conventional method) and $_r\sigma_N$ (from the proposed method) calculated from each. The graph in Fig. 4 shows the term of concentration decay on its horizontal axis and the standard deviation of uncertainty in the air exchange rate *N* on its vertical axis to plot curves for the conventional and proposed methods. The magnitude relation between the two curves indicates that the standard deviation of uncertainty is smaller for the proposed method than for the conventional method at all points. In other words, the estimation of uncertainty E_N from the conventional method is less precise than that of $_r\sigma_N$ from the proposed method. Confidence intervals are also calculated from the obtained standard deviations E_N (the conventional method) and $_r\sigma_N$ (the proposed method), and the degree of certainty supplied.

4.3. Evaluation of change in infiltration rate

We next investigated whether the discrepancy ratio β of this paper would provide an accurate evaluation in the case where the air exchange rate was changed from 0.5 (h^{-1}) to 0.4 (h^{-1}) at a point 1.25 h into a 2.5 h concentration decay. Fig. 5 shows the decay curve for this scenario. An accurate evaluation seems to have been given, with an estimation of *N* of 0.4504, and COD of 0.99657. The standard deviation of uncertainty σ_N was 0.002166, which has not captured the change in air exchange rate. The value of β was 2.3021,

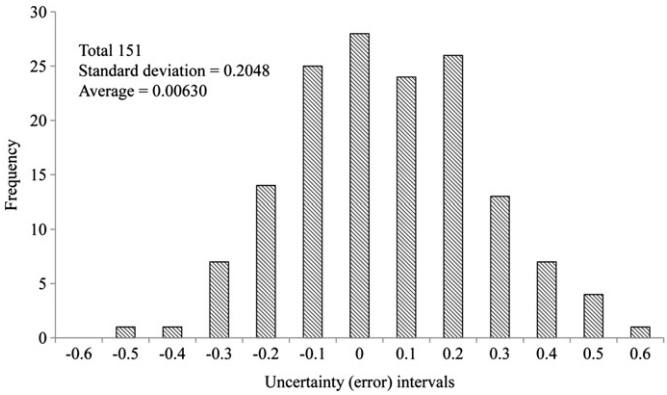

Fig. 3. Frequency distribution of measurement uncertainty (error).

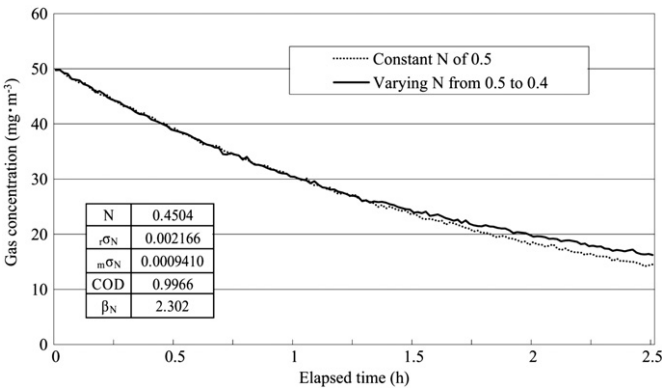

Fig. 5. Evaluation of varying air exchange rate.

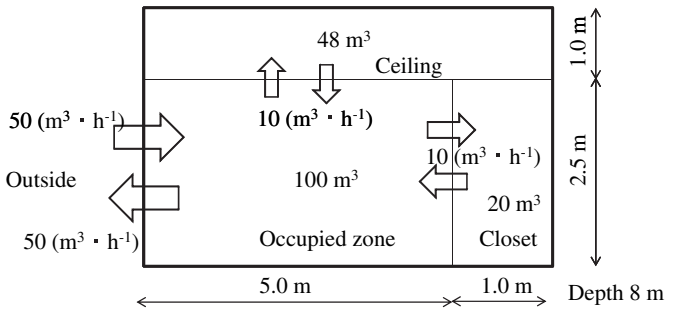

Fig. 6. Multi-zone model for non-uniformity of gas concentration. (Also used as the pseudo-non-uniform single zone model).

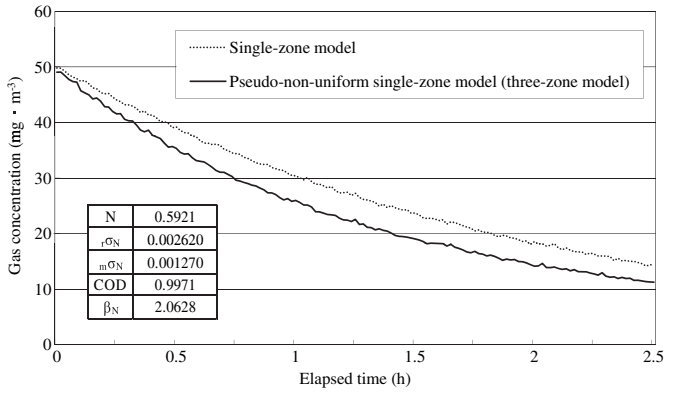

Fig. 7. Evaluation of gas concentration non-uniformity effect.

however, and this value being considerably greater than 1 indicates that some premise has not been upheld.

4.4. Evaluation of non-uniformity of concentration

One feature of the occupied zone (100 m^3) used for measurements was air exchange through a closet (20 m^3) and the ceiling (48 m^3) due to temperature differences and the like, causing insufficient uniformity of concentration between the three zones. Fig. 6 shows air flow between the three zones and the exterior atmosphere. The air flow rate between the occupied zone and outdoor was 50 ($m^3 \cdot h^{-1}$). The air flow rates between the occupied zone and the ceiling and closet were 10 ($m^3 \cdot h^{-1}$). Gas was emitted only in the occupied zone, and decay commenced once the concentration in the occupied zone reached 50 ($mg \cdot m^{-3}$). Concentration change in the occupied zone was affected in the same manner as concentrations that are not uniform. Calculations of concentration change were performed by using the heat and air flow rate network calculation program NETS[2] [13]. The time integration interval used was 30 s. Fig. 7 shows the decay of gas concentration.

The estimated air exchange rate was 0.5921 (h^{-1}). As an index of confidence assessment, the COD was 0.9971, indicating sufficiently reasonable reliability. Furthermore, the standard deviation ${}_r\sigma_N$ for uncertainty of the air exchange rate N was 0.002620, again indicating validity. The discrepancy ratio $\beta_N = 2.0628$, however, was poor, indicating that model premises were not fulfilled.

4.5. Simultaneous estimation of effective mixing volume and infiltration and evaluation of uncertainty

We performed gas emission under a single-zone model, using a sinusoidal wave with a 2-h period, and maximum and minimum flow rates of 2 and 0 ($mg \cdot s^{-1}$), respectively. Changes in gas concentration were calculated from the analytical solution of the ordinary differential equation. When doing so, system parameters v and q were 100 (m^3) and 50 ($m^3 \cdot h^{-1}$), respectively.

Fig. 8 shows a graph of the gas release rate and changes in concentration. The term used for measurements was up to 4 h elapsed time, and sampling was performed at 1-min intervals. Random numbers were generated based on the standard deviations of uncertainty $\sigma_g = 0.012$ ($mg \cdot s^{-1}$) and $\sigma_c = 0.2$ ($mg \cdot m^{-3}$), and added to the analytical solution for concentration and gas release rate as measurement error. Knowing, however, that the jaggedness or high frequency noise caused by measurement uncertainty would have a negative effect on estimation of system parameters, especially estimation of the volume, we smoothed values for cases 4.5 and 4.6 of this paper using a 10-min moving average. The length of this term can be decided by the index β and COD. Such processing is also called low pass filter and necessary for actual measurement data. When calculating the residual average as the expected values for the regression equation error used in the uncertainty propagation equation, however, the original data must be used.

Fig. 8 also shows the results of estimating parameters v and q, as well as the estimates of uncertainty. The estimation results are good, being close to the true values. The uncertainty in v and q are also appropriately evaluated as standard deviations ${}_r\sigma_v$ and ${}_r\sigma_q$. The discrepancy ratio β_N is near 1, indicating validity, as does the COD.

4.6. The relationship between sinusoidal gas emission period and effective mixing volume

We predicted that supplying excitation by sinusoidal waves with long period would allow for estimation of large effective mixing volumes that include not only the 100 (m^3) occupied space, but also the 48 (m^3) ceiling and the 20 (m^3) closet. To test this, we took the three-zone model of Section 4.4 to be a single zone with pseudo-non-uniform concentration, and tested the proposed methods for estimating v and q after performing five trials of tracer gas emission with sinusoidal period of 1, 2, 12, 24, and 48 h.

Changes in concentration were simulated using NETS with a time integration interval of 30 s, and measurement error from generated random numbers was added to pseudo-measurement values. Fig. 9 shows a graph of gas release rate and changes in concentration for the 24-h cycle. Table 1 shows estimates of v and q, standard deviation σ, discrepancy ratio β, COD, and other parameters. Excitation by longer periods approaches an effective mixing volume of 168 (m^3) and an infiltration rate of 50 ($m^3 \cdot h^{-1}$). The standard deviations of uncertainty ${}_r\sigma_v$ and ${}_r\sigma_q$ provide good estimates of the error. Furthermore, COD is approximately 1, and the discrepancy ratio β is only slightly above 1, with the exception of the 48-h cycle. From these results, we see that accuracy of estimating v and q can be increased through gas release as a sinusoidal wave with long period, even in cases where instantaneous uniform mixing of the gas within the zone is not sufficiently realized.

[2] NETS is authorized by the Ministry of Land, Infrastructure and Transport Japan as a calculation method for annual heating and cooling loads of buildings, effective 22 October 2002.

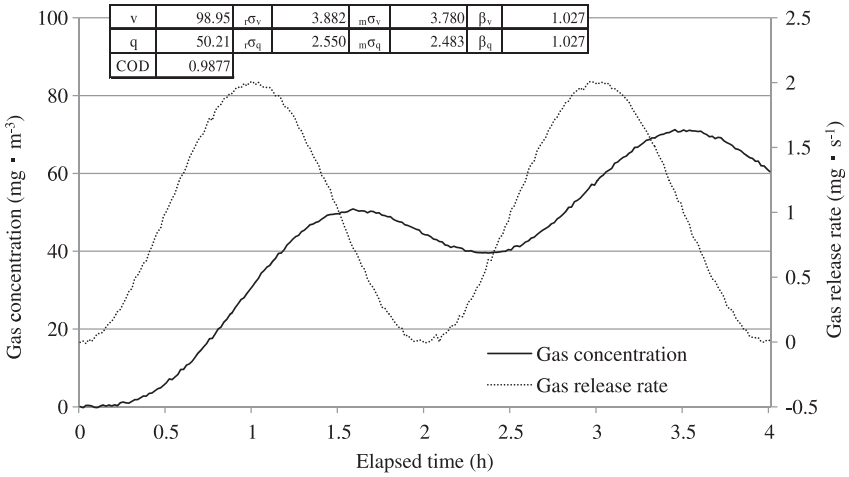

Fig. 8. Tracer gas release and concentration change (single-zone model).

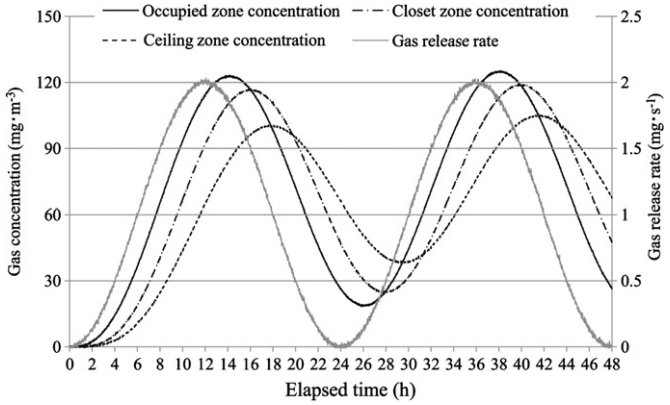

Fig. 9. Tracer gas release and concentration change (pseudo-non-uniform single-zone model).

5. Conclusions

We have re-examined and improved the method for analyzing the measurement data obtained through the conventional concentration decay method. We furthermore derived a method for simultaneous measurement of effective mixing volume and infiltration rate through measurement of gas concentration and gas supply flow rates changing as a sinusoidal wave. We verified these methods by numerical calculations for various cases. We summarize our findings as follows.

(i) We derived an equation that uses the simultaneous least-squares method for air exchange rate N from concentration measurements performed at an arbitrary time t or at times t_j equally separated by Δt.

(ii) We derived a theoretical equation for propagation from the variance of uncertainty in measured gas concentration, σ_c^2, to the variance of uncertainty in the air exchange rate, ${}_m\sigma_N^2$.

(iii) We obtained a curve of the optimal $N \cdot T_m$ that is dependent on the number of gas concentration measurement points n_p, where T_m is the term of concentration decay that minimizes uncertainty of the air exchange rate N. This curve enables the optimum term of concentration decay to be estimated. We confirmed the validity of the optimization method through calculations for various cases.

(iv) We derived an equation for propagation from regression equation error to the air exchange rate N, and other parameters, and furthermore derived an equation for calculating ${}_v\sigma_N$, the standard deviation of uncertainty in N from the residual. Graphing a comparative curve with the standard deviation E_N of the conventional method showed that the proposed method results in greater accuracy.

(v) We defined the discrepancy ratio β to serve as an indicator of fulfillment of model premises, such as the invariability of infiltration and air exchange rates, and the uniformity of gas concentration. We used case verifications to confirm that this measure is more sensitive and thus of higher utility than the coefficient of determination COD.

(vi) We derived a method for uncertainty evaluation and a least-squares-based equation for estimating the infiltration rate q and the effective mixing volume v from sinusoidal wave gas

Table 1
Relation of cycle period to effective mixing volume.

Sinusoidal cycle period (h) T	Effective mixing volume (m^3) (EMV)	Infiltration rate ($m^3 \cdot h^{-1}$)	Coefficient of determinant (COD)	Standard deviation of EMV from equation residual ${}_r\sigma_v$	Standard deviation of IR from equation residual ${}_r\sigma_q$	Standard deviation of EMV from measurement uncertainty ${}_m\sigma_v$	Standard deviation of IR from measurement uncertainty ${}_m\sigma_q$	Discrepancy ratio of EMV β_v	Discrepancy ratio of IR β_q
Case 1: 1 (h)	100.33	65.83	0.9945	6.604	7.790	5.796	6.836	1.140	1.140
Case 2: 2 (h)	101.41	62.33	0.9945	4.607	3.218	4.136	2.889	1.114	1.114
Case 3: 12 (h)	117.95	54.15	0.9816	3.509	0.758	3.372	0.729	1.041	1.041
Case 4: 24 (h)	133.44	52.35	0.9851	4.291	0.544	4.174	0.529	1.028	1.028
Case 5: 48 (h)	144.64	51.05	0.9901	5.267	0.379	5.324	0.383	0.989	0.989

emission and measurements of subsequent changes in concentration, and verified these through calculations for various cases.

(vii) We found that system identification accuracy can be improved by gas being emitted as a sinusoidal wave with long period, even in cases where instantaneous uniform mixing of the gas within the zone is not sufficient. Effective mixing volume can be regarded as a parameter for system identification that depends on the period of sinusoidal gas release.

(viii) Because high frequency noise due to uncertainty in concentration measurements would have an adverse effect on parameter estimations, it is necessary to smooth data by using a moving average. When calculating expected values for the regression equation error used in the uncertainty propagation equation, however, the original data must be used.

Acknowledgments

This research was motivated by the activities of the ISO/TC163/SC1/WG10 Committee (chair: Prof. Hiroshi Yoshino) at the Japan Testing Center for Construction Materials, in particular their investigations of ISO 12569 (Thermal performance of buildings—Determination of air change in buildings—Tracer gas dilution method). We are grateful for the advice and valuable information provided by Prof. Yoshino and the other members of the committee.

References

[1] Sherman MH, Grimsrud DT, Condon PE, Smith BV. Air infiltration measurement techniques; October 1980. Proc 1st AIC Conf (Instrumentation and Measuring Techniques), Windsor9–44.

[2] Shaw CY. The effect of tracer gas on the accuracy of air change measurements in buildings. ASHRAE Trans 1984;90(Pt 1A):212–25.

[3] Sandberg M, Blomqvist C. A quantitative estimate of the accuracy of tracer gas methods for the determination of the ventilation flow rate in buildings. Build Environ 1985;20:39–150.

[4] D'Ottavio TW, Dietz RN. Errors resulting from the use of single-zone ventilation models on multizone buildings: implications for energy conservation and indoor air quality studies. Proc ASHRAE Symp (Multi-Cell Infiltration); June 1985:777–89. Honolulu.

[5] D'Ottavio TW, Senum GI, Dietz RN. Error analysis techniques for perfluorocarbon tracer derived multizone ventilation rates. Build Environ 1988; 23:187–94.

[6] O'Neill PJ, Crawford RR. Multizone flow analysis and zone selection using a new pulsed tracer gas technique. Proc 10th AIVC Conf (Progress and Trends in Air Infiltration and Ventilation Research); September 1989:127–56. Espoo.

[7] Joint Committee for Guides in Metrology. Evaluation of measurement data - guide to the expression of uncertainty in measurement. 1st., 2008, <www.bipm.org/utils/common/documents/jcgm/JCGM_100_2008_E.pdf>; corrected version, 2010 (accessed September 2011). JCGM 100:2008 (GUM 1995 with minor corrections).

[8] ISO 12569. Thermal performance of buildings—determination of air change in buildings—tracer gas dilution method, 6.1 calculation of air change rate, p8, Annex C (informative). Confidence intervals, pp14–5, annex D (informative). 1st ed.; November 2000. Propagation of error analysis, pp. 16–7.

[9] ASTME741-95. Standard test method for determining air change in a single zone by means of a tracer gas dilution, 8.5.3.2 Optional regression method p5, X3; November 1995. Confidence intervals, p. 14, X5. Zone volume measurements with a tracer gas, p. 15.

[10] JISA1406. Method for measuring amount of room ventilation (carbon dioxide method), 3.1 Calculation method by measurement of CO_2 concentration decay; December 1974. p. 2. Revised ed.

[11] Okuyama H, Onishi Y, Tanabe S-I, Kashihara S. Statistical data analysis method for multi-zonal airflow measurement using multiple kinds of perfluorocarbon tracer gas. Build Environ 2009;44(3):546–57.

[12] Okuyama H. System identification theory of the thermal network model and an application for multi-chamber airflow measurement. Build Environ 1990; 25(4):349–63.

[13] Okuyama H. Thermal and airflow network simulation program NETS. Proc 6th Int IBPSA Conf (Building Simulation '99); September 1999:1237–44. Kyoto.

Nomenclature

N: air exchange rate (h^{-1}), hat indicates estimated N

$C(t_j)$: tracer gas concentration at elapsed time t_j for the j-th measurement in the decay process

y_j: variable representing $\log_e C(t_j)$

$\boldsymbol{Z}_j$: row matrix containing t_j and 1, $[t_j, 1]$

$\boldsymbol{a}$: vector containing system parameters to be estimated, ${}^t[-N, \log_e(0)]$, hat indicates estimated $\mathbf{a}$

e_j: regression equation error from j-th concentration measurement in decay process

n_p: total number of measurement points in concentration decay process

J_a: function for evaluating least squares in concentration decay method

Δt: measurement time interval

T: measurement term of decay method

σ_C: standard deviation of uncertainty in concentration measurement

σ_N: standard deviation of uncertainty in air exchange rate estimation

${}_m\sigma_N$: standard deviation of uncertainty in air exchange rate originating from measurement uncertainty

$N \cdot T_m$: product of air exchange rate N and uncertainty minimizing measurement term T_m

$\boldsymbol{\Lambda}_\mathbf{a}$: variance and covariance matrix for estimated parameters N and $\log_e C(t_j)$

$E(\ )$: stochastic expectation operator

${}_a\varepsilon_j$: residual of regression equation from j-th concentration measurement in decay process and the average for all ${}_a e_j$ is ${}_a\varepsilon$

${}_r\sigma_N^2$: variance of uncertainty in air exchange rate estimated using residuals from regression equation

$s(\hat{N})$: sum of residual squares for air exchange rate

s_y: total variation in air exchange rate

COD: coefficient of determination

β_N: discrepancy ratio of regression model and measurement premises for air exchange rate

v: effective mixing volume to be estimated

q: infiltration rate to be estimated

$c(t)$: tracer gas concentration in measurement of v and q

$g(t)$: tracer gas release rate in measurement of v and q

$\mathbf{p}$: vector containing v and q, ${}^t[v, q]$

g_k: time integration of $g(t)$ from $k\Delta t$ to $(k-1)\Delta t$

d_k: time integration of $\dot{c}(t)$ from $k\Delta t$ to $(k-1)\Delta t$

c_k: time integration of $c(t)$ from $k\Delta t$ to $(k-1)\Delta t$

$\mathbf{U}_k$: row matrix containing d_k and c_k, $[d_k, c_k]$

e_k: regression equation error from k-th time step measurement in system identification for v and q

J_p: evaluation function of least-squares in system identification for v and q

n_t: total time step for system identification measurement term

$\boldsymbol{\Lambda}_\mathbf{p}$: variance and covariance matrix for estimated parameters v and q

${}_p\varepsilon_k$: residual of regression equation from k-th time step measurement in system identification

${}_rE()$: stochastic expectation operator for regression equation residuals

σ_g: standard deviation of uncertainty in tracer gas releasing rate

${}_mE()$: stochastic expectation operator for measurement uncertainty

σ_{gk}^2, σ_{dk}^2, σ_{ck}^2: uncertainty variances of g_k, d_k, and c_k, respectively, calculated from measurement uncertainty

${}_r\sigma_v$, ${}_r\sigma_q$: standard deviations of uncertainty in v and q, respectively, estimated from regression equation residuals

${}_m\sigma_v$, ${}_m\sigma_q$: standard deviations of uncertainty in v and q, respectively, estimated from measurement uncertainty

β_v, β_q: discrepancy ratio for parameters v and q respectively

E_N: standard deviation of uncertainty in air exchange rate estimated by conventional methods